

Research Paper

Influence of Compression Ratio on Flywheel Dimension for a Naturally Aspirated Spark Ignition Engine: A Numerical Study

Aan Yudianto^{1,2} , Peixuan Li²¹ Automotive Engineering Education, Yogyakarta State University, Yogyakarta 55281, Indonesia² Department of Mechanical and Aerospace Engineering, Politecnico di Torino, Torino 10129, Italy aan.yudianto@uny.ac.id <https://doi.org/10.31603/ae.v3i2.3530>

Published by Automotive Laboratory of Universitas Muhammadiyah Magelang collaboration with Association of Indonesian Vocational Educators (AIVE)

Abstract

Article Info

Submitted:
03/05/2020
Revised:
22/05/2020
Accepted:
23/05/2020

The proper design of the flywheel determines in tuning the engine to confirm the better output engine performance. The aim of this study is to mathematically investigate the effect of various values of the compression ratio on some essential parameters to determine the appropriate value for the flywheel dimension. A numerical calculation approach was proposed to eventually determine the dimension of the engine flywheel on a five-cylinder four-stroke Spark Ignition (SI) engine. The various compression ratios of 8.5, 9, 9.5, 10, 10.5, and 11 were selected to perform the calculations. The effects of compression ratio on effective pressure, indicated mean effective pressure (IMEP), dynamic irregularity value of the crankshaft, and the diameter of the flywheel was clearly investigated. The study found that 2.5 increment value of the compression ratio significantly increases the effective pressure of about 41.53% on the starting of the expansion stroke. While at the end of the compression stroke, the rise of effective pressure is about 76.67%, and the changes in dynamic irregularity merely increase by about 1.79%. The same trend applies to the flywheel diameter and width, which increases 2.08% for both.

Keywords: Flywheel Dimension; Compression Ratio; Combustion Engine

Abstrak

Desain flywheel yang tepat menentukan penyetelan mesin untuk memastikan output kinerja mesin yang lebih baik. Tujuan dari penelitian ini adalah untuk menyelidiki secara matematis pengaruh berbagai rasio kompresi pada beberapa parameter penting untuk menentukan nilai yang sesuai untuk dimensi flywheel. Suatu pendekatan perhitungan numerik diusulkan untuk menentukan dimensi flywheel pada mesin Spark Ignition (SI) empat tak lima silinder. Berbagai rasio kompresi 8,5; 9; 9,5; 10; 10,5; dan 11 dipilih untuk melakukan perhitungan. Efek rasio kompresi pada tekanan efektif, indicated mean effective pressure (IMEP), nilai ketidakteraturan dinamis poros engkol, dan diameter roda gila secara jelas diselidiki. Studi ini menemukan bahwa 2,5 peningkatan nilai rasio kompresi secara signifikan meningkatkan tekanan efektif sekitar 41,53% pada awal langkah ekspansi. Sementara pada akhir langkah kompresi, kenaikan tekanan efektif adalah sekitar 76,67%, dan perubahan ketidakteraturan dinamis hanya meningkat sekitar 1,79%. Tren yang sama berlaku untuk diameter dan lebar flywheel, yang meningkat 2,08% untuk keduanya.

Kata-kata kunci: Dimensi flywheel; Rasio kompresi; Motor bakar

1. Introduction

The flywheel of an engine is utilized to regularize the speed of the crankshaft, but it does not affect the engine torque or power [1]. The

design of a flywheel should be based on the forces acting on the piston and the consequent momentum acting on the crankshaft. In the internal combustion engine, the energy is



This work is licensed under a Creative Commons Attribution-NonCommercial 4.0 International License.

developed only during the expansion stroke, which is much more than the engine load, while during the suction, compression, and exhaust stroke, there is no developed energy. The engine flywheel basically absorbs the exceeding energy during expansion stroke and releases it to the crankshaft of the engine during the other strokes. Therefore, the rotating of the crankshaft is at a relatively uniform speed. However, considering the fact when the flywheel absorbs energy, its speed increases, and it decreases during the releasing energy, the flywheel does not maintain a constant speed. The flywheel merely reduces the fluctuation of engine speed [1].

Several technological advancements have been developed and even implemented to fulfill the global requirements in terms of engine power, torque, and vehicle emission. A variable compression ratio engine is one of them, and it is a relatively new concept that is still in its nascent phase [2]. However, one of the issues related to this engine development is owing to the cost and complexity. The investigation of compression ratio effects is practically limited due to the difficulties of the design and conception of the combustion chamber, taking into account the variation of the value of the compression ratio [3]. Thus, the numerical investigation becomes practically viable with respect to these limitations.

The literature includes the numerous publications dedicated to the understanding of flywheel, the internal combustion engine, and their practical applications. Bu et al. [4] studied the design characteristic and method of flywheel motor in helicopter applications. They proposed the design method and were verified by the finite element method. Yujiang et al. [5] investigated the dynamics of a flywheel energy storage system with permanent magnetic bearing and spiral groove bearing. They compared the theoretical results and the experiment of the pendulum-tuned mass damper. Pezhman et al. [6] observed the experimental determination of the mass moment of inertia of a flywheel using dynamics and statistical methods. They developed two models for determining the mass moment of inertia and presented the benefits and drawbacks of the models. Dunne et al. [7] studied the optimal gear ratio planning for the flywheel-based kinetic energy recovery systems in motor vehicles and proposed an efficient computational methodology

for optimal gear ratio in a motor vehicle using a flywheel and continuously variable transmission. Sevik et al. [8] investigated the influence of charge motion and compression ratio on the performance of a combustion concept employing in-cylinder gasoline and natural gas blending. Hariram et al. [9] studied the influence of compression ratio on combustion and performance characteristics of a direct injection compression ignition engine and evaluated the thermal brake efficiency. The exhaust gas temperature, brake specific fuel consumption, the peak of cylinder gas pressure, ignition delay, and cumulative heat release were also investigated.

From the literature reviews, it can be inferred that a lot of research works have been conducted on the flywheel and the influence of the compression ratio on several variables. However, this present study investigates the effects of both topics and numerically calculates the influences of the compression ratio in the basic design of the flywheel in a five-cylinder engine. This study proposes the initial mathematical calculation to determine some essential parameters to determine the proper value of the flywheel dimension to ensure its functioning properly. Therefore, this will assist further research on the related topic. The outcome of these findings will also contribute to the scholars, researchers, and engineers to design with an appropriate value of the flywheel dimension. Moreover, the effect in effective pressure, indicated mean effective pressure, and dynamic irregularity of the engine crankshaft will also be investigated. The analysis in the present work is conducted considering a single steady-state engine working point on a naturally aspirated engine. In order to compute the points of the working cycle, several formulas are introduced. The Matlab software was used to perform the calculations.

2. Mathematical Description and Calculation Approach

Mathematical analysis method has been widely employed in flywheel dynamic characteristics [10], flywheel energy capacity [11], flywheel rotor control [12], flywheel dynamic modeling [13], and other related topics [14], [15]. These studies demonstrate the credibility of the method to high-potentially predicts the real condition of an engineering problem related to the

flywheel as an energy storage system. This study employs a mathematical calculation method to investigate the issue in question. The engine comprises of five-cylinder Spark-Ignition (SI) with a four-stroke engine. The compression ratio (CR) of 8.5, 9, 9.5, 10, 10.5, and 11 were selected for the study, and the calculation approach in this section is defined by the equation, data assumption and calculation sequence [16] as the following section. Before starting the calculation, several parameters and assumptions were set. **Table 1** shows the chosen engine characteristic for the calculation.

Table 1. Engine Characteristics

Parameters	Value	Unit
bore (d)	73.5	mm
stroke (c)	67	mm
crank slider parameter (λ)	0.25	-
engine speed (n)	5400	rpm
alternative masses (m_{alt}/V)	1.2	kg/dm ³
equivalent rotating masses (m_{rot}/iV)	0.85	kg/dm ³

2.1. Analysis of the indicated cycle

The indicated cycle (or actual cycle) is the actual process with the actual gas as the working fluid [17]. Therefore, the indicated cycle of the SI engine is the cycle with which the pressure-volume characteristics are studied over the four strokes of the cycle. **Figure 1** shows an ideal pressure-volume (p-V) diagram for the SI engine. Instead of the real indicated cycle, it considers a simplified air-fuel cycle with four hypotheses: Intake and exhaust valves are opened instantaneously at the dead centers; Intake and exhaust phases occur at constant pressure; Combustion and blow-down phases occur at constant volume; and Compression and expansion phases are described as polytropic transformations.

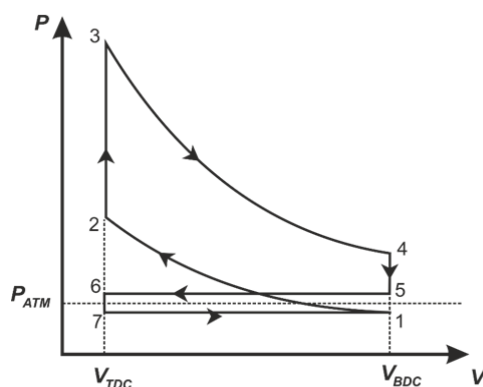


Figure 1. Indicated cycle and strokes

The graph clearly explains that the SI engine is a constant volume cycle, which is the limiting case of infinitely fast combustion at the top center (TC). It also can be seen that the volume in point 1,4, and 5 have the same value and point 2,3 and 6 also have equal values. Hereafter, it is intended to identify the value of pressure, volume, and temperature during the engine processes.

Three considerations were considered to perform the calculation of pressure and temperature at point 1. Firstly, the variation of the internal chemical energy is null since there is no chemical reaction occurring during the process. Secondly, the work done by the system through the control surface is the sum of the work done by means of the displacement of the piston plus the (negative) work done by the external environment to “push” inside the cylinder the volume of air+fuel. Thirdly, the heat exchange during the process as the heat needed to increase of 30° the temperature of the air+fuel+residuals mixture. Starting with the energy equations and substituting the expressions for the internal and the external energy changes, we obtain the following expression for the temperature at point 1.

$$T_1 = \frac{(\alpha c_{pa} + c_f)T_a + \alpha' c_p' + T_r - xr}{\alpha c_{pa} + \alpha' c_p' + c_f} + \Delta T \quad (1)$$

where α' is:

$$\alpha' = \alpha \frac{p_r}{p_a} \frac{R}{R'} \frac{T_a}{T_r} \frac{1}{\lambda_v} \frac{V_c}{V} \quad (2)$$

and the pressure p_1 is given by:

$$p_1 = p_a \left[\lambda_v (CR - 1) \frac{1 + \alpha}{\alpha} \frac{1}{RT_a} + \frac{p_r}{p_a} \frac{1}{R'T_r} \right] \frac{R_1 T_1}{CR} \quad (3)$$

The volume is calculated as:

Swept volume

$$V_d = \frac{\pi d^2 c}{4} \quad (4)$$

Clearance volume

$$V_c = \frac{V_R}{(CR - 1)} \quad (5)$$

In order to perform the calculation, the data in **Table 2** are used. The transformation from point 1 to point 2 neglects leakages, which means it has a polytropic transformation. However, the transformation cannot be considered isentropic since the heat exchange from the cylinder walls to the gas and vice-versa. In the first phase of the transformation, the temperature of the gas mixture is lower than the wall temperature T_w , therefore, the heat is transferred from the cylinder wall to the fluid.

Table 2. Data for point 1 calculation

Parameters	Value	Unit
environment pressure (p_a)	750	mmHg
environment temperature (T_a)	295	K
volumetric efficiency ($\lambda_v = m_a/m_{a,id}$)	0.82	-
residual to environment pressure ratio (p_r/p_a)	1.15	-
residual temperature (T_r)	905	K
air to fuel ratio ($\alpha_{st} = (m_a/m_b)_{st}$)	14.7	-
relative air to fuel ratio (α/α_{st})	0.95	-
fuel specific heat (c_b)	2500	J/(kg*K)
fuel vaporized fraction ($x = m_{b(vap)}/m_{b(liq)}$)	1	-
fuel vaporization heat (r)	320000	J/kg
temperature increment for the air-fuel-residual mixture during the intake stroke (ΔT)	30	°C
air elastic constant (R)	287.2	J/(kg*K)
burnt gas elastic constant (R')	288	J/(kg*K)
air-fuel-residual mixture elastic constant (R_1)	271	J/(kg*K)
air specific heat (c_p)	1009	J/(kg*K)
burnt gas specific heat (c_p')	1150	J/(kg*K)

In the second phase of the transformation, the wall is cooler than the gas, and the heat transfer is from the gas to the wall. The real transformation can be approximated by means of a polytropic equation, provided that the final point of the polytropic transformation corresponds to the final point of the real one. This is obtained by properly choosing the polytropic exponent m . In this approximation, the entropy linearly decreases from the initial point. Therefore, the coefficient m has to be lower than the exponent of the isentropic transformation ($m < 1.4$). Since the temperature, pressure, and the volume at point 1 have been calculated, the point 2 calculations depend on these and are as follows:

$$T_2 = T_1 \cdot (CR)^{(m_1-2^{-1})} \quad (6)$$

$$V_2 = V_c \quad (7)$$

$$p_2 = p_1 \cdot \left(\frac{V_2}{V_c}\right)^{m_1-2} \quad (8)$$

The necessary data for calculating point 2 is provided in **Table 3**. Point 3 in the indicated cycle graph denotes the phase when the expansion stroke starts. However, starting from the definition of the lower heating value, we consider: the presence of residuals ($\rightarrow \alpha'$); dissociation; heat exchanges by means of a reduction coefficient ($1 - \delta_A$); fuel-rich mixture: the stoichiometric fuel mass burns, while the excess fuel acts as inert. Therefore, the heating value at point 2 is

calculated from which the temperature at point 3 is found out:

$$H_{L,T_2} = H_{L,T_0} + (1 + \alpha_{st}) \cdot (c_v - c_v') \cdot (T_2 - T_0) \quad (9)$$

Thus, the temperature at point 3 is expressed by:

$$T_3 = \frac{1}{2 \cdot dq} - (c_{v3}' - 2 \cdot Td \cdot dq) + (c_{v3}' - 2 \cdot Td \cdot dq)^2 - 4 \cdot dq \{dq \cdot Td^2 - \left[\left(\frac{\alpha}{\alpha_{st}}\right) \cdot (1 - \delta A) \cdot \left(\frac{H_{L,T_2}}{1 + a + a'}\right)\right] - c_v' \cdot T_2\} \quad (10)$$

The volume and pressure are given by:

$$V_3 = V_2 \quad (11)$$

$$p_3 = \frac{p_2 \cdot T_3 \cdot R'}{T_2 \cdot R_1} \quad (12)$$

The necessary values for point 3 calculation are in **Table 4**.

Table 3. Data for the calculation of the lower heating value at T_2

Parameters	Value	Unit
compression index (m)	1.35	-
air specific heat (mean value for $H_{iv}(T_2)$ calculation under stoichiometric air to fuel ratio) (c_v)	744	J/(kg*k)
burnt gas specific heat (mean value for $H_{iv}(T_2)$ calculation under stoichiometric air to fuel ratio) (c_v')	824	J/(kg*k)
lower heating value at $T_0 = 288$ K ($H_{iv}(T_0)$)	44000	KJ/kg
T_0	288	K

Table 4. Data for point 3 calculation

Parameters	Value	Unit
dissociation heat ($\Delta Q_d = dq^*(T_3 - T_d)^2$)	-	KJ/kg
d_q	0.00054	-
T_d	1850	K
burnt gas elastic constant (R')	288	J/(kg*k)
burnt gas specific heat (c_p')	1328	J/(kg*k)
heat losses coefficient (δ_A)	0.06	-

In point 4, the transformation cannot be considered isentropic due to heat exchange from the gas to the cylinder walls ($m \neq 1.4$). In this case, since we consider the system immediately at the end of the combustion phase, in-cylinder gas is always at a higher temperature with respect to the cylinder wall. Therefore, the heat flux only occurs in one direction.

$$(T_w - T_{gas}) < 0 \rightarrow \frac{dQ}{dt} < 0 \rightarrow \text{entropy decreases} \quad (13)$$

In addition, instead of considering the real transformation, we can consider a polytropic transformation with a coefficient m' chosen. Therefore, the final point of the polytropic transformation coincides with the final point of the real transformation, since the entropy decreases: $m' < 1.4$. At point 4 from the ideal indicated cycle, the expansion process comes to an end. The p , V , T values at this point is calculated as:

$$T_4 = T_3 \cdot (CR)^{(1-m_{3-4})} \quad (14)$$

$$V_4 = V_1 \quad (15)$$

$$p_4 = p_3 \cdot CR^{-m_{3-4}} \quad (16)$$

The expansion index value of this calculation is $m' = 1.27$. Point 5, 6, and 7 calculations, based on the ideal indicated cycle shown, can be calculated in a similar way.

2.2. Indicated Mean Effective Pressure (IMEP)

IMEP is basically defined as the ratio of the indicated work produced per cycle to the cylinder volume displaced per cycle [8]. IMEP is a useful relative parameter to measure engine performance. Unlike the torque, the IMEP does not depend on the engine speed and engine size, which makes it more useful to compare engines. Even, the IMEP can be considered as one of the optimization aspects in an internal combustion engine [18]. The IMEP is used to compute the resistant momentum, which in turn is used to calculate the resistant work and the shaft work. The IMEP is thus calculated to be:

$$\begin{aligned} imep = & \left[\frac{p_1 \cdot CR \cdot (CR^{m_{1-2}} - 1)}{(CR - 1)(1 - m_{1-2})} \right] \\ & + \left[\frac{p_3 \cdot (CR^{m_{3-4}} - 1) \cdot (p_1 - pr)}{(CR - 1)(1 - m_{3-4})} \right] \end{aligned} \quad (17)$$

2.3. Effective pressure

In order to plot the effective pressure graph, it is necessary to tabulate some necessary values. The crank angle values change as the four-stroke cycle process. It is defined as the distance of the piston head from the cylinder top that varies as the crank angle varies. The designations of the four strokes for the intervals of the crank angle are expansion stroke (0-180), exhaust stroke (181-360), intake stroke (361-540), and compression stroke (541-720). The distance from the piston head from the cylinder head is calculated as:

$$x(\theta) = r \left[(1 - \cos\theta) + \frac{1}{\lambda} \left(1 - \sqrt{1 - \lambda^2 \cdot \sin^2\theta} \right) \right] \quad (18)$$

$$\lambda = \frac{\text{crank radius, } r}{\text{Connecting rod length, } l} \quad (19)$$

The swept volume is the total volume that changes according to the piston head position. It is given by:

$$V = V_c + \frac{\pi d^2}{4} \cdot x(\theta) \quad (20)$$

The gas pressure is the pressure of the combustion gases that exerts on the piston head. It varies for the four strokes as (all pressures are in KPa):

$$p_g(0 < \theta > 180) = \frac{p_4 V_1^{m_{3-4}}}{V(\theta)^{m_{3-4}}} \quad (21)$$

$$p_g(0 < \theta > 180) = p_1 \quad (22)$$

$$p_g(0 < \theta > 180) = p_5 \quad (23)$$

$$p_g(0 < \theta > 180) = \frac{p_1 V_1^{m_{1-2}}}{V(\theta)^{m_{1-2}}} \quad (24)$$

The reaction pressure p_c is the pressure that the piston exerts to counter the gas pressures exerted on it. The value of the reaction pressure is 99.99 kPa. The inertial pressure existing in the cylinder is given by:

$$i = -\frac{m_{alt}}{V} \cdot c \cdot \omega^2 \cdot r \cdot \left[\cos(\theta) + \lambda \left(\frac{\cos(2\theta)}{\cos(\beta)} \right) \right] kPa \quad (25)$$

Therefore, taking into considerations of all the pressures explained above, the effective pressure is given by:

$$p_{eff} = p_g - p_c + i \quad (26)$$

2.4. Tangential tension

The tangential tension of the SI engine depends on various parameters, such as the shaft

momentum and the tangential force experienced. The following formulas show the relation between these parameters.

$$t(\theta) = \frac{M_s 10^9}{V/2} \quad (27)$$

The shaft momentum [Nm] can be calculated from the following:

$$M_s = F_t \cdot r \cdot 10^{-3} \quad (28)$$

Therefore, the tangential force [N]:

$$F_t = p_{eff} \left(\frac{\pi d^2 \cdot 10^{-6}}{4} \right) \left(\frac{\sin(\theta + \beta)}{\cos(\beta)} \right) \quad (29)$$

2.5. Shaft and resistant tension, shaft and resistant work

It is necessary to compare the tension of the shaft and the resistant tension, as well as between the work done by the shaft and the resistant ones. Resistant work can be calculated as follow:

Resistant momentum [Nm]:

$$Mr(\theta) = \frac{imep \cdot v}{4 \cdot \pi} 10^{-6} \quad (30)$$

Because we also have the shaft momentum, we can calculate the shaft and resistant work as follow:

$$L_s(\theta) = \int_{\theta}^{4\pi} M_s(\theta) d\theta \quad [J] \quad (31)$$

$$L_r(\theta) = \int_{\theta}^{4\pi} M_r(\theta) d\theta \quad [J] \quad (32)$$

2.6. Dynamic irregularity

The dynamic irregularity of the engine crankshaft rotation influencing the operation of the flywheel is an essential measure for the flywheel design. In actual cases, there are many other considerations of dynamic effects, including other mechanical component vibrations in the engine [19]. However, this section merely considers the dynamic irregularity related to the working cycle of the engine. The dynamic irregularity is a function of the maximum and the minimum work done (shaft and resistant work) and is inversely proportional to the IMEP. It is thus expressed as:

$$\xi = \left(\frac{\Delta L_{max} + \Delta L_{min}}{imep \cdot V \cdot 10^{-6}} \right) \quad (33)$$

2.7. Instantaneous angular velocity

The instantaneous angular velocity of the engine is generally calculated with the rpm given as $((2 \cdot \pi \cdot n)/60)$, where n is the rpm.

$$\omega(\theta) = \sqrt{(\omega_0)^2 + \frac{2(L_s(\theta) - L_r(\theta))}{J}} \quad (34)$$

Where ω_{avg1} is the average angular velocity and is given by:

$$\omega_1(\theta) = \sqrt{(\omega_{avg})^2 + \frac{2(L_s(\theta) - L_r(\theta))}{J}} \quad (35)$$

$$\omega_{avg1} = \frac{1}{4\pi} \int_0^{4\pi} \omega_1(\theta) d\theta \quad (36)$$

With a specific correction factor, the real angular velocity is:

$$s = \omega_1(\theta) - \omega(\theta) \quad (37)$$

2.8. Flywheel diameter

The determination of the value of the flywheel diameter highly depends on the previous calculations. The expression to calculate the flywheel diameter is as follows.

Flywheel diameter formula is presented as:

$$d_{fly} = \sqrt[5]{\frac{320 \cdot J_{fly}}{\pi \Gamma_v}} \quad (38)$$

where,

$$J_{fly} = J_{cyl} - J_{eng} \quad (39)$$

is the inertial momentum of the flywheel.

$$J_{cyl} = \frac{\xi \cdot imep \cdot V \cdot 10^{-6}}{\delta \cdot \omega^2} \quad (40)$$

is the inertial momentum of the cylinder. (δ is the kinematic irregularity which is chosen 0.01).

$$J_{eng} = \left(\frac{m_{rot}}{i \cdot V} \right) V r^2 10^{-6} \quad (41)$$

is the inertial momentum of the engine which depend on the masses of the rotating components within.

$$\Gamma_v = 7.70 \frac{kg}{dm^3} \quad (42)$$

is the value of density from the assumed data.

With the above values, the flywheel diameter is found out. In this case, the hypothesis of the thickness of the flywheel is $0.1d_{fly}$.

3. Results and Discussion

3.1. Effective Pressure and Indicated Mean Effective Pressure

Considering Eqn. (26), it is obvious that the effective pressure depends on gas pressure, exerted pressure by the piston to encounter the gas pressure, and inertial pressure. This is interesting to graphically and numerically investigate the effects of the compression ratio to the effective pressure since it is highly related to

the compression ratio and how high the compression ratio affects on it. **Figure 2** shows the results of the effective pressure inside the engine cylinder as the function of the crank angle at the compression ratio of 8.5 to 11. Comparing the results altogether, it is clear that increasing the compression ratio of the engine affects the increment of effective pressure. Each stroke, namely expansion (0-180), exhaust (181-360), intake (361-540), and compression (541-720), is respectively depicted in the horizontal axis of the graph. When the compression ratio is equal to 8.5, the effective pressure in the starting of the expansion stroke is approximately 6113 KPa, and this value considerably increases as the compression ratio increment. For compression ratio is equal to 11, the starting effective pressure is in the order of 8652 Kpa, which means there is approximately 41.53% increment of the effective pressure value. As the crankshaft rotates, the effective pressure significantly decreases.

In the transition of the expansion stroke and exhaust stroke, there is a stepping down of the pressure because of the suddenness of the exhaust valve opening. For every variation of the compression ratios, the values are approximately 1000 KPa. During the exhaust stroke, the effective pressure is decrement. For the different compression ratio, these values are slightly different, but all values are in the order of -1000 KPa. Furthermore, the effective pressure in the

next stroke, intake, increases to the value of about 600 KPa, and it is followed by a small decrement until it finally goes back to the value of 600 KPa for CR= 8.5 and about 1060 KPa for CR=11 at the end of the compression stroke. This is clear that the 2.5-value of the compression ratio makes the changes by about 76.67% of effective pressure by the end of the compression phase of the engine. The increasing of the compression ratio does not give significant changes in the value of effective pressure apart from the beginning of the expansion stroke and the end of the compression phase.

The essential of IMEP parameters has also been studied by several researchers in some other related topics [18], [20], [21]. These studies show the needs of IMEP assessment in determining engine performance characteristics. **Table 5** and **Figure 3** explain the difference in the theoretical results of indicated mean effective pressure for all variations of the compression ratio. Considering the Eqn. (17) in the previous section, it is clear that the values of IMEP considerably increase as the compression ratio increases. This linear function starts from 1.2318×10^3 KPa when the compression value is 8.5, and it has a continuously increasing trend until the compression ratio is equal to 11, and the value of IMEP attains higher value, that is 1.3429×10^3 KPa. In every 0.5 compression ratio increment, the value of IMEP rises 0.0597×10^3 KPa in average.

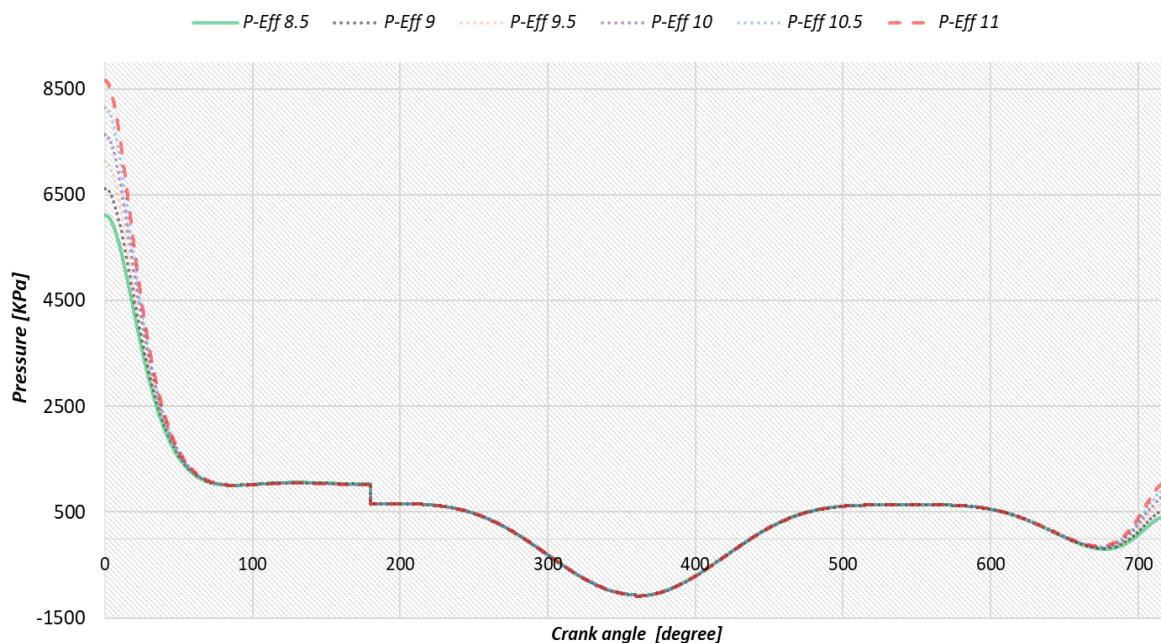
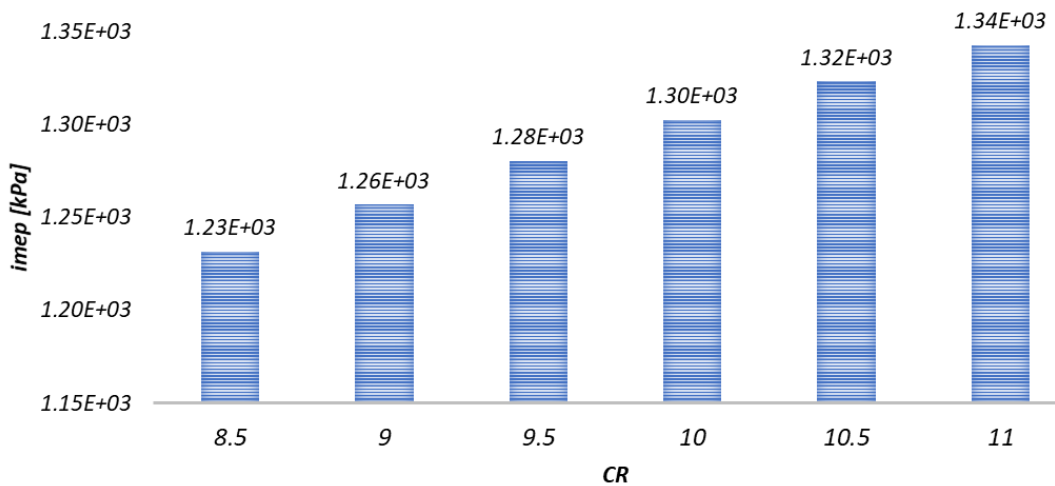


Figure 2. Effective pressure for CR = 8.5 to CR = 11.

Table 5. Indicated mean effective pressure

CR	8.5	9	9.5	10	10.5	11
IMEP (KPa)	1.2318e+03	1.2569e+03	1.2805e+03	1.3025e+03	1.3233e+03	1.3429e+03

**Figure 3.** Resulting IMEP calculation for various CR

3.2. Results of dynamic irregularity, flywheel diameters, and the flywheel width

Table 6 compares the result of dynamic irregularity (ξ) of the engine crankshaft rotation and the basic dimension of the flywheel due to the variation of the compression ratio. This dynamic irregularity becomes important since fluctuation in cyclic variations negatively affects engine performance as well [22]. Based on the Eqn. (30) and Eqn. (33) the dynamic irregularity is linearly proportional to shaft and resistance work, but it is inversely proportional to the IMEP. However, shaft and resistance work is determined by the resistance momentum, which also depends on the IMEP. It, however, gives a correlation for each other. The IMEP itself depends on the compression ratio and on the condition in every point in the indicated cycle, and the final results of the dynamic irregularity are depicted in Table 6. As such, the more the compression ratio, the more the dynamic irregularity of the engine crankshaft rotation. When the compression ratio is 8.5, the result of the dynamic irregularity calculation is 0.9617, and for an engine with a compression ratio is equal to 11, the result of the dynamic irregularity is 0.9789. The effect of the chosen compression ratio gives a less significant rise in the value of dynamic irregularity, which is merely about 1.79%.

In order to determine the flywheel diameter, it is compulsory to find the results of the inertial

momentum of the flywheel for the five-cylinder engine based on the Eqn. (41). It depends on the value of the dynamic irregularity and also IMEP. In this case, the chosen kinematic irregularity is 0.01. The mass of the rotating component is determined as 7.7 kg/dm³ as explained in Eqn. (38). Therefore, after observing the expressions, the compression ratio eventually determines the flywheel dimension. The compression ratio determines the condition of the points in the indicated cycle of the engine, which finds out the IMEP and effective pressure. Furthermore, it has a correlation in the tangential tension, resistance momentum, dynamic irregularity, and finally, it determines the flywheel diameter.

Based on the specification and assumed values, the compression ratio equals to 8.5 yields in 268.3 mm of flywheel diameter while for 11 compression ratio results in the 273.9 mm flywheel diameter. The width of the flywheel is 26.83 mm for 8.5 compression ratio and 27.39 for CR equal to 11. The increasing values of flywheel diameter and flywheel width are at the same value of 2.08%. These are based on the hypothesis that the width of the flywheel is 10% of the flywheel diameter. The more compression ratio, the bigger the flywheel diameter. This dimension is the initial value references to further design the flywheel serving as kinetic energy storage and retrieval devices. The proper analytical calculation should be performed appropriately so

that the flywheel is also able to retrieve the energy to deliver high output power at high rotational velocity as the potentially emerging energy storage technology in today's world.

Table 6. Flywheel diameter and width

Compression Ratio	ξ	Diameter (mm)	Width (mm)
8.5	0.9617	268.3	26.83
9	0.9654	269.6	26.96
9.5	0.9689	270.8	27.08
10	0.9723	271.9	27.19
10.5	0.9756	272.9	27.29
11	0.9789	273.9	27.39

4. Conclusion

The influence of the compression ratio on the five-cylinder SI engines was clearly examined in this study over the entire numerical calculations at the various value of the compression ratio. The engine compression ratio determined the value of the pressures and temperatures in the indicated cycle, which, furthermore, defined the value of the IMEP and effective pressure. The value of the effective pressure was necessary to calculate shaft momentum, while IMEP was useful to determine the resistance momentum. These two values were needed to compute shaft and resistance work, which, next, these were used to find the value of the dynamic irregularity that, together with IMEP and angular velocity, determined the value of the inertial momentum of the flywheel. Finally, the flywheel diameter was calculated by the value of the inertial momentum and the masses of the rotating component. By following this procedure, it is concluded that the more compression ratio of the engine, the more dynamic irregularity experienced by the engine, and as an impact, the more diameter of the flywheel is needed. The 2.5 increasing value of CR enormously increases the effective pressure of 41.53% on the initial phase of the expansion stroke. At the end of the compression stroke, the progression of effective pressure is about 76.67%, and the alterations on dynamic irregularity merely rise about 1.79%. The identical trend occurs for the value of flywheel diameter and width, which equally increases by 2.08%. Further studies are, therefore, to conduct the calculation of the flywheel diameter for a multi-cylinder engine. It is also planned to perform the study on the effect of engine rpm to

the result of the engine parameter such as IMEP and dynamic irregularity.

Acknowledgment

Gratitude and appreciation are expressed to the *Lembaga Pengelola Dana Pendidikan* (LPDP) for the full funding of graduate degree education, *Politecnico di Torino* for the complete support of this work and Yogyakarta State University as the current affiliation.

Nomenclature

α	air
c	stroke
c	constant
c_p	air specific heat
c_p'	burnt gas specific heat
d	bore, diameter, dissociation
F_t	tangential force
f	fuel
H	air specific heat
H_{iv}	lower heating value
i	number of cylinders
J	inertial momentum
L	work
M	momentum
m	mass, compression index
n	engine speed
p	pressure
R	universal gas constant
R'	burnt gas elastic constant
r	specific heat of vaporation, residual
s	specific correction factor
T	Temperature
t	tangential
V	volume
w	wall
x	fuel vaporized fraction
δ	kinematic irregularity
δ_A	thermal losses term
i	inertial pressure
ω	angular velocity
x	piston distance from the top center
λ	crank slider parameter
λ_v	volumetric efficiency
ξ	dynamic irregularity
Γ_v	masses of the rotating component
dq	loss term
rpm	revolution per minute
st	stoichiometric
ATM	atmosphere

BDC	Bottom Dead Center
CR	Compression Ratio
IMEP	Indicated mean effective pressure
SI	Spark Ignition
TDC	Top Dead Center
TC	Top Center

Author's Declaration

Authors' contributions and responsibilities

The authors made substantial contributions to the conception and design of the study. The authors took responsibility for data analysis, interpretation and discussion of results. The authors read and approved the final manuscript.

Funding

This research was funded by LPDP scholarship, Ministry of Finance - Republic of Indonesia.

Availability of data and materials

All data are available from the authors.

Competing interests

The authors declare no competing interest.

Additional information

No additional information from the authors.

References

- [1] R. S. Khurmi and J. K. Gupta, *A Textbook of Machine Design*, First Edit. New Delhi: Eurasia Publishing House LTD, 2004.
- [2] R. Thomas, M. Sreesankaran, J. Jaidi, D. M. Paul, and P. Manjunath, "Experimental evaluation of the effect of compression ratio on performance and emission of SI engine fuelled with gasoline and n-butanol blend at different loads," *Perspect. Sci.*, 2016, doi: 10.1016/j.pisc.2016.06.076.
- [3] F. Hadia, S. Wadhah, H. Ammar, and O. Ahmed, "Investigation of combined effects of compression ratio and steam injection on performance, combustion and emissions characteristics of HCCI engine," *Case Stud. Therm. Eng.*, 2017, doi: 10.1016/j.csite.2017.07.005.
- [4] J. Bu, M. Zhou, X. Lan, and K. Lv, "Design characteristic and method of the flywheel motor of cihfape used in helicopter," in *ASME 2017 Internal Combustion Engine Division Fall Technical Conference, ICEF 2017*, 2017, doi: 10.1115/ICEF20173543.
- [5] Y. Qiu and S. Jiang, "Dynamics of Flywheel Energy Storage System with Permanent Magnetic Bearing and Spiral Groove Bearing," *J. Dyn. Syst. Meas. Control. Trans. ASME*, 2018, doi: 10.1115/1.4037297.
- [6] P. Hassanpour, M. Weaser, R. Colquhoun, K. Alghemlas, and A. Alrashdan, "Experimental determination of the mass moment of inertia of a flywheel using dynamics and statistical methods," in *ASME International Mechanical Engineering Congress and Exposition, Proceedings (IMECE)*, 2015, doi: 10.1115/IMECE2015-53557.
- [7] J. F. Dunne and L. A. Ponce Cuspinera, "Optimal gear ratio planning for flywheel-based kinetic energy recovery systems in motor vehicles," *J. Dyn. Syst. Meas. Control. Trans. ASME*, 2015, doi: 10.1115/1.4029929.
- [8] J. Sevik *et al.*, "Influence of charge motion and compression ratio on the performance of a combustion concept employing in-cylinder gasoline and natural gas blending," *J. Eng. Gas Turbines Power*, 2018, doi: 10.1115/1.4040090.
- [9] V. Hariram and R. Vagesh Shangar, "Influence of compression ratio on combustion and performance characteristics of direct injection compression ignition engine," *Alexandria Eng. J.*, 2015, doi: 10.1016/j.aej.2015.06.007.
- [10] L. Chen, W. K. Shi, and Z. Y. Chen, "Modeling and Experimental Study on Dynamic Characteristics of Dual-Mass Flywheel Torsional Damper," *Shock Vib.*, 2019, doi: 10.1155/2019/5808279.
- [11] D. V. Berezhnoi, L. R. Gajnulina, and A. A. Sachenkov, "Investigation of stress-strain state in the flywheel and estimation their specific energy capacity," *MATEC Web Conf.*, vol. 129, pp. 1–4, 2017, doi: 10.1051/mateconf/201712906027.
- [12] Y. Ren and J. Fang, "Modified cross feedback control for a magnetically suspended flywheel rotor with significant gyroscopic effects," *Math. Probl. Eng.*, 2014, doi: 10.1155/2014/325913.
- [13] L. Chen, R. Zeng, and Z. Jiang, "Nonlinear dynamical model of an automotive dual

- mass flywheel," *Adv. Mech. Eng.*, 2015, doi: 10.1177/1687814015589533.
- [14] M. Andriollo, R. Benato, and A. Tortella, "Design and modeling of an integrated flywheel magnetic suspension for kinetic energy storage systems," *Energies*, 2020, doi: 10.3390/en13040847.
- [15] A. Yudianto, N. Kurniadi, I. Wayan Adiyasa, and Z. Arifin, "The Effect of Masses in the Determination of Optimal Suspension Damping Coefficient," in *Journal of Physics: Conference Series*, 2019, vol. 1273, no. 1, doi: 10.1088/1742-6596/1273/1/012067.
- [16] A. Mittica and S. Ambrosio, "Combustion Engines and Their Application to Vehicles - Lecture notes," in *Combustion Engines and Their Application to Vehicles*, Torino: Politecnico di Torino, 2018.
- [17] J. Heywood, *Internal Combustion Engine Fundamentals*. McGraw-Hill, 1998.
- [18] F. K. Ma *et al.*, "Parameter optimization on the uniflow scavenging system of an OP2S-GDI engine based on indicated mean effective pressure (IMEP)," *Energies*, 2017, doi: 10.3390/en10030368.
- [19] M. Cocconcelli *et al.*, "Numerical and Experimental Dynamic Analysis of IC Engine Test Beds Equipped with Highly Flexible Couplings," *Shock Vib.*, 2017, doi: 10.1155/2017/5802702.
- [20] G. M. Kosmadakis and C. D. Rakopoulos, "A fast CFD-based methodology for determining the cyclic variability and its effects on performance and emissions of spark-ignition engines," *Energies*, 2019, doi: 10.3390/en12214131.
- [21] J. Hunicz, "On cyclic variability in a residual effected HCCI engine with direct gasoline injection during negative valve overlap," *Math. Probl. Eng.*, 2014, doi: 10.1155/2014/359230.
- [22] O. I. Awad, Z. Zhang, M. Kamil, X. Ma, O. M. Ali, and S. Shuai, "Wavelet analysis of the effect of injection strategies on cycle to cycle variation GDI optical engine under clean and fouled injector," *Processes*, 2019, doi: 10.3390/pr7110817.